ELSEVIER

Journal of Alloys and Compounds 227 (1995) 44–48

Journal of ALLOYS AND COMPOUNDS

# Characterization of novel ternary uranium silicides and germanides with the $U_2Mo_3Si_4$ structure type in the U–(Mo, W, V)–(Si, Ge) systems

T. Le Bihan, H. Noël

*Laboratoire de Chimie du Solide et Inorganique Moléculaire, URA CNRS 1495, Université de Rennes I, Avenue du Général Leclerc, 35042 Rennes Cédex, France*

Received 17 February 1995

**Abstract**

Novel compounds, $U_2W_3Si_4$, $U_2Mo_3Ge_4$ and $U_2V_3Ge_4$, have been synthesised by argon arc melting, using the correct elemental compositions. The crystal structures of $U_2W_3Si_4$ ($a=6.847(5)$ Å, $b=6.858(1)$ Å, $c=6.767(9)$ Å, $\beta=109.77(1)°$) and of $U_2Mo_3Ge_4$ ($a=7.016(4)$ Å, $b=6.995(2)$ Å, $c=6.949$ Å, $\beta=110.21(2)°$) have been determined from single-crystal X-ray data. They have been shown to be isotypic with $U_2Mo_3Si_4$ ($a=6.876(3)$ Å, $b=6.883(1)$ Å, $c=6.760(3)$ Å, $\beta=109.79(2)°$, space group $P2_1/c$, $Z=2$). From X-ray powder intensity data, $U_2V_3Ge_4$ ($a=6.986(1)$ Å, $b=6.976(1)$ Å, $c=6.927(1)$ Å, $\beta=109.94(2)°$) was found to crystallize in the same structure type. $U_2V_3Ge_4$ is ferromagnetic below $T_C=60$ K whereas $U_2W_3Si_4$, $U_2Mo_3Si_4$ and $U_2Mo_3Ge_4$ do not show any ferromagnetic transition at low temperature.

*Keywords:* Crystal structure; Magnetic properties; Ternary uranium silicides; Ternary uranium germanides

## 1. Introduction

The compound $U_2Mo_3Si_4$ has a structural type which was first reported by Sikiritsa et al. in 1978 [1], but no detailed data are available concerning the crystallographic and magnetic properties for this compound. In our search for new uranium-based highly correlated electron compounds, we have investigated the ternary U–Mo–Si system which includes $U_2Mo_3Si_4$. We have looked for similar compounds of uranium with germanium and with other transition metals of columns V and VI.

This paper describes the preparation, structural chemistry and magnetic behaviour of the compounds $U_2Mo_3Si_4$, $U_2W_3Si_4$, $U_2Mo_3Ge_4$ and $U_2V_3Ge_4$.

## 2. Experimental

The compounds $U_2Mo_3Si_4$, $U_2Mo_3Ge_4$ and $U_2V_3Ge_4$ were synthesized by directly arc melting the three elements under argon atmosphere. Owing to the high melting point of tungsten compared with that of uranium, $U_2W_3Si_4$ was prepared in two steps: formation of a W–Si alloy was followed by melting with U metal. To ensure homogeneity, the arc-melted buttons were flipped over and remelted twice. The weight losses were below 1 mass%. To allow the heat treatment to reach an equilibrium state, the buttons were wrapped in a tantalum foil and annealed under vacuum in an induction furnace for 10 h at 1350 °C. Attempts to synthesize "$U_2W_3Ge_4$" and "$U_2V_3Si_4$" were unsuccessful.

Small single crystals of $U_2Mo_3Si_4$, $U_2W_3Si_4$ and $U_2Mo_3Ge_4$ were obtained by heating the arc-melted button at a temperature of about 1450 °C for the molybdenum compounds whereas $U_2W_3Si_4$ was heated at 1500 °C for 8 h, followed by slow cooling. The same technique, when applied to $U_2V_3Ge_4$, did not reveal any significant growth of the microcrystals which were preformed in the arc melting process.

## 3. Structural chemistry

Single-crystal X-ray diffraction was performed on an automatic Enraf-Nonius CAD-4 four-circle diffractometer with Mo $K\alpha$ radiation ($\lambda=0.71069$ Å). The lattice parameters were obtained by least-squares refinement of the setting angles of 25 reflections and from powder data refinements in the case of $U_2V_3Ge_4$ ($a=6.986(1)$ Å, $b=6.979(1)$ Å, $c=6.927(1)$ Å, $\beta=109.94(2)°$). Details of the intensity data collection and the crystallographic data are summarized in Table 1.


*SSDI* 0925-8388(95)01628-7

Table 1
Crystallographic data for $U_2Mo_3Si_4$, $U_2W_3Si_4$ and $U_2Mo_3Ge_4$

| Composition | $U_2Mo_3Si_4$ | $U_2W_3Si_4$ | $U_2Mo_3Ge_4$ |
|---|---|---|---|
| Space group | $P2_1/c$, number 14, origin at $\bar{1}$ | $P2_1/c$, number 14, origin at $\bar{1}$ | $P2_1/c$, number 14, origin at $\bar{1}$ |
| Lattice parameters [a] | $a=6.876(3)$ Å<br>$b=6.883(1)$ Å<br>$c=6.760(3)$ Å<br>$\beta=109.79(2)°$ | $a=6.847(5)$ Å<br>$b=6.858(1)$ Å<br>$c=6.767(9)$ Å<br>$\beta=109.77(1)°$ | $a=7.016(4)$ Å<br>$b=6.995(2)$ Å<br>$c=6.949(4)$ Å<br>$\beta=110.21(2)°$ |
| Cell volume (Å$^3$) | $V=301.1(2)$ | $V=299.0(4)$ | $V=320.1(2)$ |
| Formula units per cell | $Z=2$ | $Z=2$ | $Z=2$ |
| Formula weight (g) [f] | $M=876.22$ | $M=1139.95$ | $M=1054.23$ |
| Calculated density (Mg m$^{-3}$) | 9.66 | 12.66 | 10.94 |
| Crystal size (mm$^3$) | $0.08\times0.09\times0.08$ | $0.13\times0.14\times0.15$ | $0.10\times0.10\times0.10$ |
| Scan range | $1°\leqslant\theta\leqslant30°$ | $1°\leqslant\theta\leqslant40°$ | $1°\leqslant\theta\leqslant30°$ |
| Range in *hkl* | $-9;+9;+9$ | $+12;+12;-12$ | $-9;+9;+9$ |
| Linear absorption coefficient (Mo K$\alpha_1$) (mm$^{-1}$) | 57.45 | 110.62 | 71.49 |
| Total number of reflections | 1017 | 2076 | 1066 |
| Reflections with $I>3\sigma(I)$ | 782 | 1451 | 825 |
| Goodness of fit | 2.044 | 2.117 | 1.012 |
| Conventional residual (F) | $R_F=0.074$ | $R_F=0.053$ | $R_F=0.028$ |
| Weighted residual ($w=1/\sigma^2(F)$) | $R_w=0.089$ | $R_w=0.068$ | $R_w=0.035$ |

[a] From CAD 4.

Table 2
Atom parameters [a] for $U_2Mo_3Si_4$, $U_2W_3Si_4$ and $U_2Mo_3Ge_4$

| Compound | Atom | Position | *x* | *y* | *z* | *B* (Å$^2$) | $\beta_{11}$ | $\beta_{22}$ | $\beta_{33}$ | $\beta_{12}$ | $\beta_{13}$ | $\beta_{23}$ |
|---|---|---|---|---|---|---|---|---|---|---|---|---|
| $U_2Mo_3Si_4$ | U | 4e | 0.1896(1) | 0.1676(1) | 0.0590(1) | 0.51(1) | 0.0026(1) | 0.0018(1) | 0.0034(1) | 0.0003(2) | −0.0012(2) | 0.0000(2) |
| | Mo(1) | 2d | 1/2 | 0 | 1/2 | 0.61(4) | 0.0029(4) | 0.0026(4) | 0.0041(4) | −0.0008(7) | −0.0008(6) | −0.0002(7) |
| | Mo(2) | 4e | 0.2442(3) | 0.6631(2) | 0.2523(3) | 0.64(3) | 0.0020(3) | 0.0020(3) | 0.0048(3) | −0.0000(4) | −0.0006(4) | −0.0006(4) |
| | Si(1) | 4e | 0.0902(8) | 0.9543(7) | 0.3686(8) | 0.43(8) | 0.0030(8) | 0.0017(8) | 0.0002(8) | −0.003(1) | −0.006(1) | −0.002(1) |
| | Si(2) | 4e | 0.5037(8) | 0.3668(8) | 0.3673(9) | 0.53(8) | 0.0030(8) | 0.0019(8) | 0.0033(9) | −0.001(2) | −0.001(1) | 0.002(2) |
| $U_2W_3Si_4$ | U | 4e | 0.1888(1) | 0.1675(1) | 0.0585(1) | 0.77(1) | 0.0048(1) | 0.0040(1) | 0.0047(1) | 0.0004(1) | 0.0032(1) | 0.0002(1) |
| | W(1) | 2d | 1/2 | 0 | 1/2 | 0.80(1) | 0.0047(1) | 0.0043(1) | 0.0049(1) | −0.0006(2) | 0.0033(2) | −0.0001(2) |
| | W(2) | 4e | 0.2454(1) | 0.6628(1) | 0.2520(1) | 0.88(1) | 0.0052(1) | 0.0044(1) | 0.0056(1) | −0.0001(2) | 0.0031(1) | −0.0004(2) |
| | Si(1) | 4e | 0.0857(7) | 0.9539(8) | 0.3660(8) | 0.96(7) | 0.0062(7) | 0.0049(7) | 0.0054(7) | −0.000(1) | 0.0033(1) | −0.002(1) |
| | Si(2) | 4e | 0.5047(7) | 0.3674(8) | 0.3693(7) | 0.84(6) | 0.0046(6) | 0.0047(7) | 0.0053(6) | −0.001(1) | 0.0033(9) | 0.002(1) |
| $U_2Mo_3Ge_4$ | U | 4e | 0.1890(1) | 0.1682(1) | 0.0535(1) | 0.83(1) | 0.0048(1) | 0.0042(1) | 0.0048(1) | 0.0002(1) | 0.0033(1) | −0.0001(1) |
| | Mo(1) | 2d | 1/2 | 0 | 1/2 | 0.86(2) | 0.0052(2) | 0.0045(2) | 0.0049(2) | −0.0009(4) | 0.0040(3) | 0.0008(4) |
| | Mo(2) | 4e | 0.2443(1) | 0.6550(2) | 0.2531(2) | 0.95(2) | 0.0052(2) | 0.0049(2) | 0.0056(2) | 0.0003(3) | 0.0030(3) | −0.0005(3) |
| | Ge(1) | 4e | 0.0933(2) | 0.9504(2) | 0.3621(2) | 0.92(2) | 0.0053(2) | 0.0049(2) | 0.0054(2) | −0.0000(4) | 0.0038(3) | −0.0004(4) |
| | Ge(2) | 4e | 0.5071(2) | 0.3611(2) | 0.3644(2) | 0.93(2) | 0.0056(2) | 0.0049(2) | 0.0052(2) | −0.0007(4) | 0.0040(3) | −0.0006(4) |

[a] $B=(4/3)\Sigma_{i,j}\beta_{i,j}a_ia_j$. The coefficients for anisotropic thermal measurements are expressed as $\exp(-h^2\beta_{11}+k^2\beta_{22}+l^2\beta_{33}+hk\beta_{12}+hl\beta_{13}+kl\beta_{23})$. Standard deviations in the least-significant digits are given in parentheses.

The structures when solved were found to be in the space group $P2_1/c$ (number 14). Intensities were corrected for Lorentz and polarization effects and were further corrected for absorption in the final stages of the refinements by means of the DIFABS program [2]. All the calculations were carried out using the SDP crystallographic software [3] installed on a MicroVAX 3100 computer. The structure of $U_2Mo_3Si_4$ was refined first. The position of the uranium (4e (*x*,*y*,*z*)) was determined by the Patterson method. Difference Fourier analysis revealed the Wyckoff positions 2d ($\frac{1}{2}$,0,$\frac{1}{2}$) and 4e (*x*,*y*,*z*) for molybdenum and 4e (*x*,*y*,*z*) for silicon. These results (Table 2) are in agreement with those reported by Bodak et al. [4] on the rare-earth-based analogues of $U_2Mo_3Si_4$.

For $U_2W_3Si_4$ and $U_2Mo_3Ge_4$, the positions of all the atoms were assigned by analogy with those of $U_2Mo_3Si_4$. For all the compounds, the refinements were performed using a full-matrix least-squares calculation which included a site population analysis. There was no indication of any significant deviation from full occupancies. Furthermore a difference Fourier analysis gave no indication for the occupancy of further atomic sites. The final residual value and the final positional and thermal parameters are listed in Table 1 and

Table 3
Interatomic distances (Å) for $U_2Mo_3Si_4$, $U_2W_3Si_4$ and $U_2Mo_3Ge_4$

| $U_2Mo_3Si_4$ | | $U_2W_3Si_4$ | | $U_2Mo_3Ge_4$ | |
|---|---|---|---|---|---|
| Atoms | Distance | Atoms | Distance | Atoms | Distance |
| U–1Si(2) | 2.800(4) | U–1Si(2) | 2.811(5) | U–1Ge(2) | 2.853(1) |
| U–1Si(1) | 2.823(4) | U–1Si(1) | 2.823(5) | U–1Ge(1) | 2.892(1) |
| U–1Si(2) | 2.876(4) | U–1Si(2) | 2.861(5) | U–1Ge(2) | 2.941(1) |
| U–1Si(2) | 2.880(4) | U–1Si(2) | 2.872(5) | U–1Ge(1) | 2.953(1) |
| U–1Si(1) | 2.881(4) | U–1Si(1) | 2.881(5) | U–1Ge(2) | 2.963(1) |
| U–1Si(1) | 2.910(4) | U–1Si(1) | 2.884(5) | U–1Ge(1) | 2.994(1) |
| U–1Si(1) | 2.999(4) | U–1Si(1) | 2.971(5) | U–1Ge(1) | 3.000(1) |
| U–1Mo(2) | 3.185(1) | U–1W(2) | 3.182(1) | U–1Mo(2) | 3.190(1) |
| U–1Mo(2) | 3.230(1) | U–1W(2) | 3.222(1) | U–1Mo(2) | 3.292(1) |
| U–1Mo(1) | 3.235(1) | U–1W(1) | 3.235(1) | U–1Mo(1) | 3.294(1) |
| U–1Mo(1) | 3.245(0) | U–1W(1) | 3.237(1) | U–1Mo(1) | 3.331(1) |
| U–1U | 3.368(1) | U–1U | 3.567(1) | U–1U | 3.429(1) |
| U–2U | 3.565(0) | U–2U | 2.985(1) | U–2U | 3.658(1) |
| Mo(1)–2Si(2) | 2.639(4) | W(1)–2Si(2) | 2.649(5) | Mo(1)–2Ge(2) | 2.697(1) |
| Mo(1)–2Si(1) | 2.671(4) | W(1)–2Si(2) | 2.674(5) | Mo(1)–2Ge(1) | 2.701(1) |
| Mo(1)–2Si(2) | 2.682(4) | W(1)–2Si(1) | 2.689(5) | Mo(1)–2Ge(2) | 2.702(1) |
| Mo(1)–2Mo(2) | 3.046(1) | W(1)–2W(2) | 3.034(1) | Mo(1)–2Mo(2) | 3.109(1) |
| Mo(1)–2Mo(2) | 3.049(1) | W(1)–2W(2) | 3.037(1) | Mo(1)–2Mo(2) | 3.140(1) |
| Mo(1)–2U | 3.235(1) | W(1)–2U | 3.235(1) | Mo(1)–2U | 3.294(1) |
| Mo(1)–2U | 3.245(0) | W(1)–2U | 3.237(1) | Mo(1)–2U | 3.331(1) |
| Mo(2)–1Si(1) | 2.514(4) | W(2)–1Si(1) | 2.519(5) | Mo(2)–1Ge(1) | 2.554(2) |
| Mo(2)–1Si(2) | 2.564(4) | W(2)–1Si(2) | 2.553(5) | Mo(2)–1Ge(2) | 2.602(2) |
| Mo(2)–1Si(2) | 2.577(4) | W(2)–1Si(2) | 2.563(5) | Mo(2)–1Ge(2) | 2.630(2) |
| Mo(2)–1Si(1) | 2.578(4) | W(2)–1Si(1) | 2.570(5) | Mo(2)–1Ge(1) | 2.644(2) |
| Mo(2)–1Si(1) | 2.598(4) | W(2)–1Si(1) | 2.594(5) | Mo(2)–1Ge(1) | 2.657(2) |
| Mo(2)–1Si(2) | 2.648(4) | W(2)–1Si(2) | 2.633(5) | Mo(2)–1Ge(2) | 2.691(2) |
| Mo(2)–1Mo(1) | 3.046(1) | W(2)–1W(1) | 3.034(1) | Mo(2)–1Mo(1) | 3.109(1) |
| Mo(2)–1Mo(1) | 3.049(1) | W(2)–1W(1) | 3.037(1) | Mo(2)–1Mo(1) | 3.140(1) |
| Mo(2)–1U | 3.185(1) | W(2)–1U | 3.182(1) | Mo(2)–1U | 3.190(1) |
| Mo(2)–1U | 3.230(1) | W(2)–1U | 3.222(1) | Mo(2)–1U | 3.292(1) |
| Si(1)–1Mo(2) | 2.514(4) | Si(1)–1W(2) | 2.519(5) | Ge(1)–1Mo(2) | 2.554(2) |
| Si(1)–1Si(1) | 2.566(0) | Si(1)–1Si(1) | 2.551(0) | Ge(1)–1Mo(2) | 2.664(2) |
| Si(1)–1Mo(2) | 2.578(4) | Si(1)–1W(2) | 2.570(5) | Ge(1)–1Mo(2) | 2.657(2) |
| Si(1)–1Mo(2) | 2.598(4) | Si(1)–1W(2) | 2.594(5) | Ge(1)–1Mo(1) | 2.701(1) |
| Si(1)–1Mo(1) | 2.671(4) | Si(1)–1W(1) | 2.689(5) | Ge(1)–1Ge(1) | 2.757(0) |
| Si(1)–1U | 2.823(4) | Si(1)–1U | 2.823(5) | Ge(1)–1U | 2.892(1) |
| Si(1)–1U | 2.881(4) | Si(1)–1U | 2.881(5) | Ge(1)–1U | 2.953(1) |
| Si(1)–1U | 2.910(4) | Si(1)–1U | 2.884(5) | Ge(1)–1U | 2.994(1) |
| Si(1)–1U | 2.999(4) | Si(1)–1U | 2.971(5) | Ge(1)–1U | 3.000(1) |
| Si(2)–1Mo(2) | 2.564(4) | Si(2)–1W(2) | 2.553(5) | Ge(2)–1Mo(2) | 2.602(2) |
| Si(2)–1Mo(2) | 2.577(4) | Si(2)–1Si(2) | 2.554(10) | Ge(2)–1Mo(2) | 2.630(2) |
| Si(2)–1Si(2) | 2.578(8) | Si(2)–1W(2) | 2.563(5) | Ge(2)–1Mo(2) | 2.691(2) |
| Si(2)–1Mo(1) | 2.639(4) | Si(2)–1W(2) | 2.633(5) | Ge(2)–1Mo(1) | 2.697(1) |
| Si(2)–1Mo(2) | 2.648(4) | Si(2)–1W(1) | 2.649(5) | Ge(2)–1Mo(1) | 2.702(1) |
| Si(2)–1Mo(1) | 2.682(4) | Si(2)–1W(1) | 2.674(5) | Ge(2)–1Ge(2) | 2.733(3) |
| Si(2)–1U | 2.800(4) | Si(2)–1U | 2.811(5) | Ge(2)–1U | 2.853(1) |
| Si(2)–1U | 2.876(4) | Si(2)–1U | 2.861(5) | Ge(2)–1U | 2.941(1) |
| Si(2)–1U | 2.880(4) | Si(2)–1U | 2.872(5) | Ge(2)–1U | 2.963(1) |

Table 2 respectively. Selected interatomic distances are gathered in Table 3.

The crystal structure of $U_2Mo_3Si_4$ is shown in Fig. 1. Uranium atoms are surrounded by seven silicon atoms forming a pentagonal bipyramid. The shortest U–U distance is 3.368 Å which is below the Hill limit [5] and indicates a significant 5f–5f orbital overlap. Four molybdenum atoms are situated at a U–Mo distance somewhere between 3.18 and 3.25 Å. Two molybdenum atoms, Mo(1) and Mo(2), have six neighbouring silicon atoms, in an octahedral coordination for Mo(1) atoms. The two silicon atoms are in tetrakisdecahedral coordination polyhedrons which represent trigonal tricapped prisms.

The substitution of germanium by silicon leads to a larger unit cell for $U_2Mo_3Ge_4$, with an increase of all interatomic distances, particularly between the uranium atoms ($d$(U–U) = 3.429 Å). This implies some 5f localization in going from the silicide to the germanide. Conversely, the inter-

Table 4
Magnetic data for $U_2Mo_3Si_4$, $U_2W_3Si_4$, $U_2Mo_3Ge_4$ and $U_2V_3Ge_4$

| Compound | Ferromagnetic order temperature (K) | $\mu_{eff}$ ($\mu_B$) | $\Theta_p$ (K) | $\chi_0$ ($\times 10^{-3}$ cm$^3$ mol$^{-1}$) |
|---|---|---|---|---|
| $U_2Mo_3Si_4$ | – | 2.30 | −240 | 1.39 |
| $U_2W_3Si_4$ | – | 2.73 | −560 | 0.99 |
| $U_2Mo_3Ge_4$ | – | 2.86 | −136 | 0.77 |
| $U_2V_3Ge_4$ | 60 | 2.38 | 41 | 2.45 |

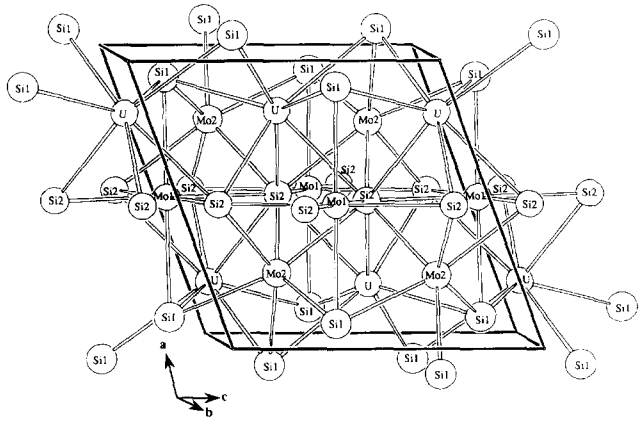


Fig. 1. Crystal structure of $U_2Mo_3Si_4$.

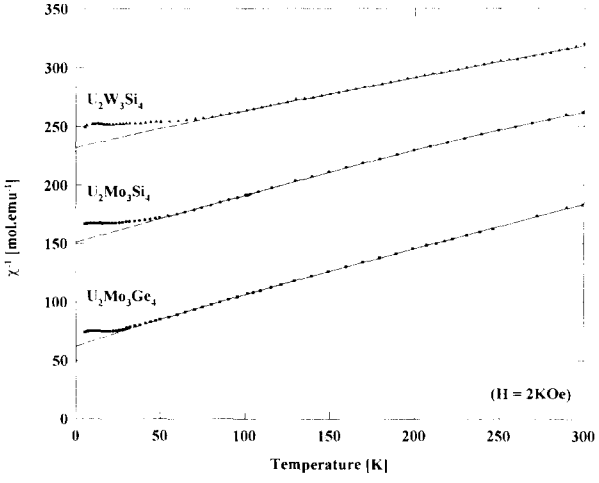


Fig. 2. Reverse susceptibility vs. temperature for $U_2W_3Si_4$, $U_2Mo_3Si_4$ and $U_2Mo_3Ge_4$.

atomic distances are shorter in $U_2W_3Si_4$ than in $U_2Mo_3Ge_4$ and the rather short U–U distance (3.348 Å) falls far below the Hill limit, indicating a large 5f delocalization in this compound.

## 4. Magnetism

The magnetic properties of these compounds have been studied using a SQUID magnetometer in the temperature

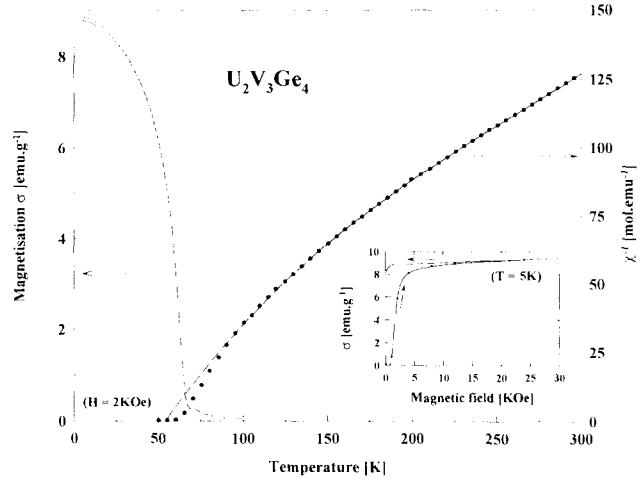


Fig. 3. Magnetization (left-hand scale) and reciprocal susceptibility (right-hand scale) vs. temperature for $U_2V_3Ge_4$. Magnetization vs. field is also shown.

range 2–300 K and in fields up to 30 kOe. These properties are summarized in Table 4 and Figs. 2 and 3.

Fig. 2 shows the temperature dependence of the reciprocal susceptibility for $U_2W_3Si_4$, $U_2Mo_3Si_4$ and $U_2Mo_3Ge_4$. All three compounds show very similar behaviour with temperature-independent (Van-Vleck-type) paramagnetism below 50 K, 30 K and 25 K respectively. The susceptibility was fitted according to the modified Curie–Weiss law at higher temperatures. The value of the susceptibility is the highest for $U_2Mo_3Ge_4$ throughout the entire temperature range. It decreases along the series of the three compounds with increasing 5f delocalization (as deduced from the contraction of the interatomic U–U distances, which was calculated during the crystal structure refinements).

Fig. 3 shows the magnetic behaviour of $U_2V_3Ge_4$. It is different from the previous members of the series. This compound exhibits ferromagnetic interactions with an ordering temperature of $T_C \approx 60$ K. The magnetization becomes saturated below 20 kOe with a magnetization reaching $0.68\mu_B/U$ (see inset in Fig. 3). As no magnetic order was observed in the other isotypic compounds, we suspect that the onset of long-range magnetic ordering in $U_2V_3Ge_4$ results from the influence of the vanadium. However, the low value of the effective magnetic moment (Table 4) is not consistent with

this conclusion. Neutron diffraction experiments are being undertaken to solve its magnetic structure.

## References

[1] M. Sikiritsa, L.G. Aksel'rud and Ya.P. Yarmolyuk, Crystal structure of the compound $U_2Mo_3Si_4$, *Abstr. 3rd Conf. of Union on Intermetallic Compound Crystallochemistry,* Vishcha Shkola, L'vov, 1978, p. 11 (in Russian).

[2] N. Walker and D. Stuart, *Acta Crystallogr. A, 39* (1983) 158.

[3] B.A. Frenz, Enraf Nonius CAD-4 SDP, in H. Schlenk, R. Olthof-Hazekamp, H. Von Konigsveld and G.C. Bassy (eds.), *Computing in Crystallography,* Delft University Press, Delft, 1978, p. 64.

[4] O.I. Bodak, Yu.K. Gorelenko, V.I. Yarovets and R.V. Skolozdra, *Izv. Akad. Nauk. SSSR, Neorg. Mater., 20* (5) (1984) 853.

[5] H.H. Hill, in W.N. Miner (ed.), *Plutonium 1970 and Other Actinides,* AIME, New York, 1970, p. 2.